ANTIMICROBIAL AGENTS AND CHEMOTHERAPY, Dec. 2000, p. 3456–3460 Vol. 44, No. 12
0066-4804/00/$04.00+0

Structural and Topological Differences between a Glycopeptide-Intermediate Clinical Strain and Glycopeptide-Susceptible Strains of *Staphylococcus aureus* Revealed by Atomic Force Microscopy

SUSAN BOYLE-VAVRA,[1]* JONGIN HAHM,[2] S. J. SIBENER,[2] AND ROBERT S. DAUM[1]

Department of Pediatrics[1] and Department of Chemistry and The James Franck Institute,[2] The University of Chicago, Chicago, Illinois 60637

Received 2 May 2000/Returned for modification 18 July 2000/Accepted 15 September 2000

Novel cell surface topography was revealed on cocci from a glycopeptide-intermediate *Staphylococcus aureus* (GISA) clinical strain by using atomic force microscopy. The GISA isolate and its revertant had two parallel circumferential surface rings. One equatorial surface ring was observed in control strains. In vancomycin-susceptible strains, additional rings were formed in the presence of vancomycin. Ring depth measurements also revealed striking differences between the GISA strain and susceptible strains grown with or without vancomycin.

The emerging problem of intermediate resistance to the glycopeptide antibiotic vancomycin in *Staphylococcus aureus* isolates (25) has raised concern, since few therapeutic options remain for treatment. Glycopeptide antibiotics kill gram-positive bacteria by interfering with the synthesis of peptidoglycan (reviewed in reference 1a). We reasoned that the identification of cell surface alterations associated with the resistance phenotype could lead to an improved understanding of the mechanism of resistance. Studies performed to date to describe the morphology of untreated and vancomycin-treated vancomycin-resistant *S. aureus* cells (7, 8, 13, 20–22) have been limited to the examination of ultrathin cross-sections of fixed bacteria using transmission electron microscopy. Characterization of the cell surface topology of glycopeptide-resistant isolates is still lacking.

Atomic force microscopy (AFM), a scanning probe microscopy technique recently used to elucidate the detailed nanoscale structure of soft polymers (11, 12), has recently been used to elucidate the detailed structure of biological surfaces (15), including the cell walls of bacteria (3, 4, 26). The advantages of AFM over alternative techniques such as scanning electron microscopy include enhanced resolution, the ability to measure surface topographic features, and sample preparation lacking harsh chemical treatments that might form artifacts.

Using contact mode AFM, we characterized the surface topology of cells from a glycopeptide intermediate-resistant *S. aureus* (GISA) isolate (strain NJ) (5, 6, 23). For strain NJ, the MIC of vancomycin is intermediate according to the guidelines published by the National Committee for Clinical Laboratory Standards (18). A vancomycin-susceptible revertant of that isolate (NJ[P15]) (2) was also studied, as well as two vancomycin-susceptible control strains, RN4220 (14) and methicillin-resistant *S. aureus* (MRSA) isolate 6/3 8N, which was obtained from our collection (24). The effects of vancomycin induction on surface topology were also examined.

* Corresponding author. Mailing address: Department of Pediatrics, The University of Chicago MC 6054, 5841 S. Maryland Ave., Chicago, IL 60637. Phone: (773) 702-6401. Fax: (773) 702-1196. E-mail: sboyleva@midway.uchicago.edu.

Bacteria were collected from brain heart infusion agar (BHIA) and suspended in 0.85% saline to an A_{600} of 1.0. A 5.0-μl drop of the bacterial suspension was applied to a small glass chip (4 by 4 mm^2) and allowed to air dry. The subinhibitory concentration of vancomycin for each strain was determined by passaging on a series of BHIA plates containing vancomycin (1 to 8 μg/ml). AFM imaging was performed in contact mode with a Topometrix Discoverer AFM (Thermomicroscopes, Sunnyvale, Calif.) equipped with a 75-μm scanner and a silicon nitride cantilever probe (spring constant of 0.032 N/m). The cantilever probe exerted a constant force of 1 nN on the surfaces of the bacterial cells. The same cantilever tip was used for all experiments; however, force calibration measurements of the cantilever probe were performed prior to the scanning of each new sample.

When samples were scanned over a large area, cocci were arranged in grapelike clusters, the morphology typical of staphylococci (Fig. 1). The mean cell diameter was consistent with that expected for *S. aureus* (1 μm). The cell surface of the cocci appeared relatively smooth in texture, except for an occasional protrusion. Viewing cells of strains RN4220 and 6/3 8N over a small scanning area revealed a single equatorial ring on the surface of each cell (Fig. 2a). This ring likely marks the septal plane of division between future daughter cells. Tetrads of undivided cells were occasionally seen with their rings forming two perpendicular lines, as in a cross-like structure (Fig. 2b), a morphology demonstrated previously by scanning electron microscopic imaging of freeze-etched samples (9). Such images illustrate *S. aureus* division septa forming normally at right angles (10).

When grown on medium containing a subinhibitory concentration of vancomycin (1 μg/ml), vancomycin-susceptible control strains RN4220 and 6/3 8N often produced cells with additional grooves or rings which either were nearly parallel (referred to hereafter as parallel) or intersected the primary ring at various angles (Fig. 2c). In contrast, untreated cells of strain NJ (Fig. 3a) produced a pair of circumferential rings arranged in parallel. Revertant strain NJ[P15] also had the parallel, dual-ring topology (Fig. 3b). When strain NJ was grown in the presence of a subinhibitory concentration of vancomycin (7 μg/ml) (Fig. 3c and e), the cells maintained the

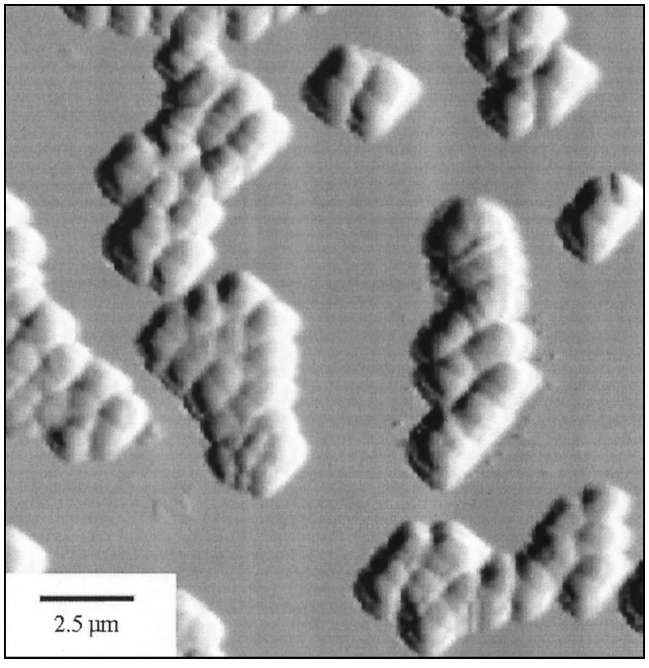

FIG. 1. AFM image of GISA strain NJ showing cocci arranged in grapelike clusters. Scanning area, 25 by 25 μm.

parallel dual-ring topology. In contrast, vancomycin at 3 μg/ml induced cells of strain NJ[P15] to produce a third ring (Fig. 3d and f) that was parallel to the two primary circumferential rings seen on untreated cocci. Interestingly, although colonial growth of strain NJ[P15] did not arise on BHIA containing 7 μg of vancomycin/ml, cells did grow in small, flat, patchy films on the agar surface. Interestingly, cells from this film also produced three rings, identical to those of cells that produced colonies at 3 μg of vancomycin/ml.

The depth of the circumferential rings was the characteristic that best distinguished the resistant from the susceptible strains. When cells were grown in the absence of vancomycin, the grooves that formed the rings on cells of strain NJ were shallower than those of cells of the three vancomycin-susceptible strains examined (Table 1). The grooves deepened on cells of all of the strains when they were grown in the presence of vancomycin (Table 1); however, the increase was slightly more pronounced for the susceptible revertant strain (4.5-fold increase) than for the resistant parent (3.4-fold).

The two parallel rings on untreataed cells from strain NJ were separated by a narrower gap (164 ± 13.4 nm, mean gap width ± the standard deviation) than that between parallel rings on untreated cells from the revertant strain NJ[P15] (190 ± 19 nm). The mean width of the gap between parallel rings of strain NJ grown in the presence of 7 μg of vancomycin/ml was 167 ± 10 nm. Thus, vancomycin did not considerably affect the distance between the rings of cells of the resistant strain. For the revertant strain NJ[P15] grown in the presence of vancomycin (3 μg/ml), the three parallel rings were separated by two consecutive gaps with mean widths of 198 ± 17 nm (large gap) and 169 ± 15 nm (small gap). Thus, the width of the large interring gap on vancomysin-treated cells of strain NJ[P15] corresponds to that found between the two rings of the untreated cells of this strain.

To summarize, as shown in the schematic in Fig. 4, one equatorial ring was present on cells from the vancomycin-susceptible strains, whereas a dual-ring structure characterized

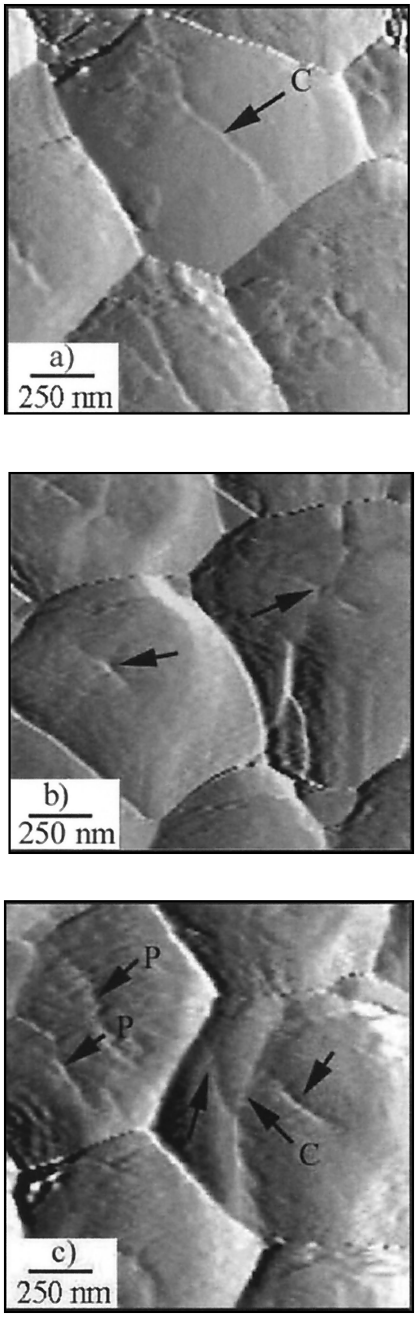

FIG. 2. AFM images of cocci from vancomycin-susceptible control strains. (a) Vancomycin-susceptible MRSA strain 6/3 8N showing a typical view of a single circumferential ring (arrow). (b) Undivided tetrad of cells of strain RN4220 with the perpendicular arrangement of circumferential rings forming a cross-like structure (arrow). (c) Cells of vancomycin (1 μg/ml)-treated, vancomycin-susceptible MRSA strain 6/3 8N illustrating an equatorial, circumferential ring (arrow labeled C) with aberrantly placed grooves (unlabeled arrows) formed in response to vancomycin. Arrows labeled P indicate nearly parallel grooves formed in one cell. Scanning area, 1.5 by 1.5 μm.

the cell surface of GISA strain NJ. The dual-ring topography of strain NJ is not associated with the methicillin resistance phenotype of the isolate, since cells of the vancomycin-susceptible, methicillin-resistant control strain had only one ring. Strain NJ had the shallowest ring depth of the four strains examined, and only vancomycin-resistant strain NJ was resis-

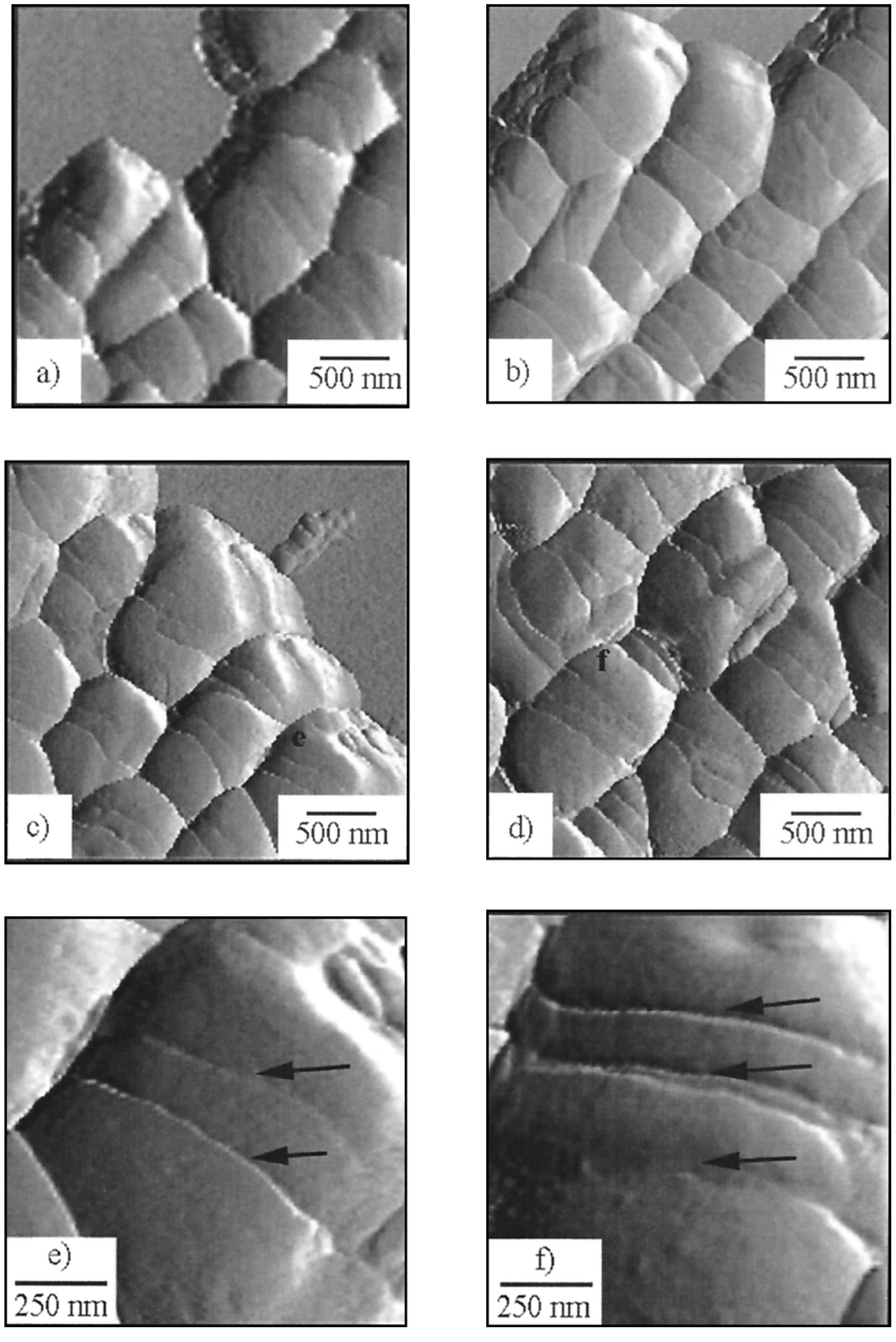

FIG. 3. AFM images of cells from GISA clinical strain NJ and related revertant strain NJ[P15] showing parallel rings traversing each cell. Panels: a, GISA strain NJ; b, revertant strain NJ[P15]; c, vancomycin (7 μg/ml)-treated cells of strain NJ; d, vancomycin (3 μg/ml)-treated cells of strain NJ[P15]; e, closer-range view of the cell labeled e in panel c; f, closer-range view of the cell labeled f in panel d. The arrows in panels e and f point to nearly parallel rings. The scanning area used to obtain the images in panels a to d was 3 by 3 μm. The scanning area used to obtain the images shown in panels e and f was 1 by 1 μm.

TABLE 1. Mean depths of circumferential rings observed in vancomycin-susceptible strains and GISA clinical strain NJ[a]

Strain (resistance phenotype)	Mean ring depth (nm) ± SD	
	Untreated	Vancomycin treated
RN4220 (Vm^s)	9.8 ± 2.52	21.50 ± 6.26
6/3 8N (Vm^s Mc^r)	9.28 ± 2.62	21.97 ± 4.58
NJ[P15] (Vm^s Mc^r)	9.7 ± 1.45	44.4 ± 4.46
NJ (Vm^r Mc^r)	5.7 ± 2.3	19.5 ± 2.1

[a] Values represent the mean measurements of eight cells chosen at random. Phenotypes: Vm^r, vancomycin resistant (signifies a vancomycin MIC of at least 8 μg/ml); Vm^s, vancomycin susceptible; Mc^r, methicillin resistant. Subinhibitory vancomycin concentrations varied among the strains; strain NJ was grown in the presence of 7 μg of vancomycin/ml, NJ[P15] was grown in the presence of 3 μg of vancomycin/ml, and RN4220 and 6/3 8N were grown in the presence of 1 μg of vancomycin/ml.

tant to further ring or groove formation in the presence of vancomycin.

From these data, we can envision that the susceptible progenitor of strain NJ formed additional grooves when exposed to vancomycin and that cells with the parallel dual-ring structure had a selective advantage in the presence of vancomycin. The dual-ring structure of the revertant form of strain NJ was apparently inherited from the resistant parent strain, and reversion was likely obtained through a pathway that utilized a second-site mutation that did not abolish formation of the second ring. At present, however, it is difficult to assess whether or not these observations represent a general phenomenon that occurs in all GISA strains.

The circumferential ring seen by AFM imaging is likely the site of the bacterial septum. Septum formation is a complex process requiring the coordinated targeting of a number of cell division proteins (16). We can speculate that the second equatorial ring of strain NJ was formed by aberrant targeting of *S. aureus* cell division proteins that are normally arranged at the cell surface in one equatorial ring (1, 10, 17, 27). Alternately, the dual rings can be explained by thickening of cross walls. The latter explanation is unlikely since evidence for uniform cross wall thickening in this strain is lacking from our transmission electron microscopic images of thin sections (unpublished data).

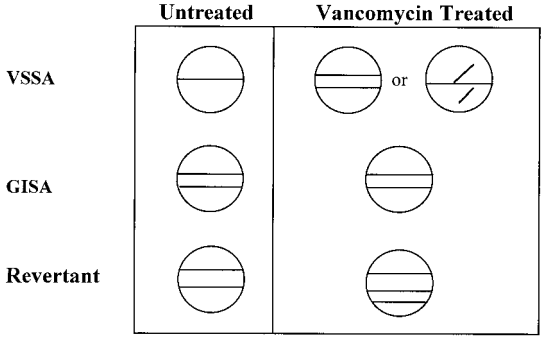

FIG. 4. Schematic illustrating patterns of rings and grooves in untreated and vancomycin-treated *S. aureus* strains. Vancomycin-susceptible *S. aureus* (VSSA) control strains produced a single circumferential ring in untreated cells, and additional grooves or rings with various orientations were present in vancomycin (1 μg/ml)-treated control cells. Untreated cells of the GISA strain NJ (GISA) and the revertant isolate had two parallel rings. Vancomycin (7 μg/ml)-treated cells of the GISA strain had the same appearance as untreated cells. Vancomycin (3 μg/ml)-treated cells of the revertant strain produced a third ring. Note that the two adjacent gaps between rings on the vancomycin-treated revertant strain are unequal in size.

In conclusion, the fine structural detail provided by AFM has extended previous topographic studies of vancomycin-susceptible (8) and vancomycin-resistant *S. aureus* (7, 8, 13, 19–22) by showing novel morphological changes occurring in the cell surface in untreated, as well as vancomycin-treated, staphylococci.

We are grateful to Fred Tenover from the Centers for Disease Control and Prevention for providing the NJ GISA isolate.

This work was supported by NIAID grants RO3 1 AI 44999-0 and RO1 AI40481-01A1 and a grant from the Grant Healthcare Foundation (Lake Forest, Ill.). This work was also supported by the NSF-Materials Research Science and Engineering Center at The University of Chicago (DMR-9808595).

REFERENCES

1. **Baba, T., and O. Schneewind.** 1998. Targeting of muralytic enzymes to the cell division site of Gram-positive bacteria: repeat domains direct autolysin to the equatorial surface ring of *Staphylococcus aureus*. EMBO J. **17:**4639–4646.
1a. **Barna, J. C. J., and D. H. Williams.** 1984. The structure and mode of action of glycopeptide antibiotics of the vancomycin group. Annu. Rev. Microbiol. **38:**339–357.
2. **Boyle-Vavra, S., S. K. Berke, J. C. Lee, and R. S. Daum.** 2000. Reversion of glycopeptide resistance phenotype in *Staphylococcus aureus* clinical isolates. Antimicrob. Agents Chemother. **44:**272–277.
3. **Braga, P. C., and D. Ricci.** 1998. Atomic force microscopy: application to investigation of *Escherichia coli* morphology before and after exposure to cefodizime. Antimicrob Agents Chemother. **42:**18–22.
4. **Braga, P. C., and D. Ricci.** 2000. Detection of rokitamycin-induced morphostructural alterations in *Helicobacter pylori* by atomic force microscopy. Chemotherapy **46:**15–22.
5. **Centers for Disease Control and Prevention.** 1997. *Staphylococcus aureus* with reduced susceptibility to vancomycin—United States, 1997. Morbid. Mortal. Weekly Rep. **46:**765–766.
6. **Centers for Disease Control and Prevention.** 1997. Update: *Staphylococcus aureus* with reduced susceptibility to vancomycin—United States, Sept. 1997. Morbid. Mortal. Weekly Rep. **46:**813–815.
7. **Daum, R. S., S. Gupta, R. Sabbagh, and W. M. Milewski.** 1992. Characterization of *Staphylococcus aureus* isolates with decreased susceptibility to vancomycin and teicoplanin: isolation and purification of a constitutively produced protein associated with decreased susceptibility. J. Infect. Dis. **166:**1066–1072.
8. **Filice, G., P. Lanzarini, P. Orsolini, L. Soldini, L. Perversi, G. Carnevale, G. Comolli, and F. Castelli.** 1990. Effect of teicoplanin and vancomycin on *Staphylococcus aureus* ultrastructure. Microbiologica **13:**231–237.
9. **Giesbrecht, P., H. Labischinski, and J. Wecke.** 1985. A special morphogenetic wall defect and the subsequent activity of "murosomes" as the very reason for penicillin-induced bacteriolysis in staphylococci. Arch. Microbiol. **141:**315–324.
10. **Giesbrecht, P., J. Wecke, and B. Reinicke.** 1976. On the morphogenesis of the cell wall of staphylococci. Int. Rev. Cytol. **44:**225–318.
11. **Hahm, J., W. Lopes, H. Jaeger, and S. Sibener.** 1998. Defect evolution in ultrathin films of polystyrene-block-polymethylmethacrylate diblock copolymers observed by atomic force microscopy. J. Chem. Physics **109:**10111–10114.
12. **Hahm, J., and S. Sibener.** 2000. Cylinder alignment in annular structures of microphase-separated polystyrene-β-poly(methylmethacrylate). Langmuir **16:**4766–4769.
13. **Hanaki, H., K. Kuwahara-Arai, S. Boyle-Vavra, R. S. Daum, H. Labischinski, and K. Hiramatsu.** 1998. Activated cell-wall synthesis is associated with vancomycin resistance in methicillin-resistant *Staphylococcus aureus* clinical strains Mu3 and Mu50. J. Antimicrob. Chemother. **42:**199–209.
14. **Kreiswirth, B. N., S. Lofdahl, M. J. Betley, M. O'Reilly, P. M. Schlievert, M. S. Bergdoll, and R. P. Novick.** 1983. The toxic shock syndrome exotoxin structural gene is not detectably transmitted by a prophage. Nature **305:**709–712.
15. **Lal, R., and S. A. John.** 1994. Biological applications of atomic force microscopy. Am. J. Physiol. **266:**C1–C21.
16. **Lutkenhaus, J.** 1998. The regulation of bacterial cell division: a time and place for it. Curr. Opin. Microbiol. **1:**210–215.
17. **Lutkenhaus, J., and S. G. Addinall.** 1997. Bacterial cell division and the Z ring. Annu. Rev. Biochem. **66:**93–116.
18. **National Committee for Clinical Laboratory Standards.** 1999. Performance standards for antimicrobial susceptibility testing, ninth informational supplement M100–S9, vol. 19. National Committee for Clinical Laboratory Standards, Wayne, Pa.
19. **Pfeltz, R. F., V. K. Singh, J. L. Schmidt, M. A. Batten, C. S. Baranyk, M. J. Nadakavukaren, R. K. Jayaswal, and B. J. Wilkinson.** 2000. Characterization of passage-selected vancomycin-resistant *Staphylococcus aureus* strains of

diverse parental backgrounds. Antimicrob. Agents Chemother. **44:**294–303.
20. **Sieradzki, K., R. B. Roberts, S. W. Haber, and A. Tomasz.** 1999. The development of vancomycin resistance in a patient with methicillin-resistant *Staphylococcus aureus* infection. N. Engl. J. Med. **340:**517–523.
21. **Sieradzki, K., and A. Tomasz.** 1996. A highly vancomycin-resistant laboratory mutant of *Staphylococcus aureus*. FEMS Microbiol. Lett. **142:**161–166.
22. **Sieradzki, K., and A. Tomasz.** 1997. Inhibition of cell wall turnover and autolysis by vancomycin in a highly vancomycin-resistant mutant of *Staphylococcus aureus*. J. Bacteriol. **179:**2557–2566.
23. **Smith, T. L., M. L. Pearson, K. R. Wilcox, C. Cruz, M. V. Lancaster, B. Robinson-Dunn, F. Tenover, M. J. Zervos, J. D. Band, E. White, and W. R. Jarvis.** 1999. Emergence of vancomycin resistance in *Staphylococcus aureus*. N. Engl. J. Med. **340:**493–501.
24. **Suggs, A. H., M. C. Maranan, S. Boyle-Vavra, and R. S. Daum.** 1999. Methicillin-resistant and borderline methicillin-resistant asymptomatic *Staphylococcus aureus* colonization in children without identifiable risk factors. Pediatr. Infect. Dis. J. **18:**410–414.
25. **Tenover, F. C.** 1999. Implications of vancomycin-resistant *Staphylococcus aureus*. J. Hosp. Infect. **43**(Suppl.)**:**S3–S7.
26. **Umeda, A., M. Saito, and K. Amako.** 1998. Surface characteristics of gram-negative and gram-positive bacteria in an atomic force microscope image. Microbiol. Immunol. **42:**159–164.
27. **Yamada, S., M. Sugai, H. Komatsuzawa, S. Nakashima, T. Oshida, A. Matsumoto, and H. Suginaka.** 1996. An autolysin ring associated with cell separation of *Staphylococcus aureus*. J. Bacteriol. **178:**1565–1571.